Proceedings of ISFOG 2025
5TH INTERNATIONAL SYMPOSIUM ON
FRONTIERS IN OFFSHORE GEOTECHNICS
Nantes, France | June 9-13 2025

ISBN 978-2-85782-758-0

Modelling pullout of suction buckets under varying rates

D. Bhakta*
The University of Melbourne, Melbourne, Australia

A. Roy, S.H. Chow
The University of Melbourne, Melbourne, Australia

H. Zhou
Norwegian Geotechnical Institute, Perth, Australia

**debiprasad.bhakta@student.unimelb.edu.au (corresponding author)*

ABSTRACT: Suction bucket jacket is one of the major foundation types being adopted for supporting offshore wind turbines. With combined effects of increasing water depths and environmental loads and more optimised bucket size, the tensile capacity of the bucket may become a critical design issue. In this study, a parametric study has been carried out through numerical modelling to investigate the uplift performance of a suction bucket in sand considering a range of pullout rates, thus drainage conditions. In order to capture the key constitutive behaviour of the sand relevant to the problem of interest, an advanced bounding surface constitutive model, termed SANISAND-F, has been employed. This model can not only replicate the shear induced dilation of dense sands realistically, but also account for the effect of in-situ fabric effects. Additionally, coupled fluid-mechanical interaction analysis is also necessary in order to model partial drainage conditions. In this paper, the performance of the numerical model was first validated against centrifuge test results. Then a series analyses were performed by vertically pulling out the bucket at a range of velocities to cover the entire drainage regime from undrained, partially drained to drained conditions. The results of the analyses show significant effect of the drainage conditions on the uplift performance of the bucket and provide valuable insights into the underlying mechanisms which explains why the pullout behaviour varies under different drainage conditions. Associated interaction between fabric orientation and loading direction in different drainage conditions has also been discussed.

Keywords: Suction bucket; Numerical modelling; Sand; SANISAND-F; Fabric anisotropy

1 INTRODUCTION

Suction bucket jacket is one of the major foundation types being adopted for supporting offshore wind turbines, especially in relatively greater water depths, due to its simplicity and environment-friendly installation. Due to its multi-leg jacket configuration, the overturning moment from the top structure is re-distributed among the legs with a "push-pull" mechanism. The windward buckets may experience tension if the pull overtakes the vertical downward force, while the leeward buckets are in compression. With combined effects of increasing water depth and environmental loads and more optimised (reduced) bucket size, the tensile capacity of the foundation may become a critical design aspect. Therefore, significant research effort is required to enable more reliable prediction of bucket performance under tensile loads.

This is especially important for the buckets installed in sands, for which the tensile capacity under undrained conditions may not be possible to be fully mobilised due to fast dissipation of negative excess pore pressures (suction) relative to the loading rate. Furthermore, even if the bucket has sufficient ultimate uplift capacity, it is still necessary to evaluate the accumulate upward displacement of the bucket due to intermittent tensile loads throughout its lifetime, in order to limit the tilt of the jacket foundation system.

In addition to physical modelling tests, such as those reported in Senders (2008), Gutz and Achmus (2021) and da Silva Pereira et al. (2023), numerical modelling provides a powerful alternative. However, the reliability and accuracy of the numerical modelling largely depends on the capability of the constitutive model in replicating the relevant behaviour of sand. Simple elastoplastic models, such as Mohr-Coulomb model, are not deemed to be adequate. More advanced models, such as hypoplastic model used by Achmus and Thieken (2014), DeltaSand by Ayyilmaz et al. (2023), and SANISAND by Shen et al. (2017) are considered to be necessary, in combination with sufficient and careful calibration.

In this paper, a numerical study is carried out to investigate the effect of partial drainage on the pullout capacity of suction buckets using SANISAND-F model (Petalas et al., 2020) with a coupled fluid-mechanical interaction framework. This also allows a thorough assessment of the model performance in

boundary value problem, and the results provided insights on the relative fabric orientation for different pullout rates and associated drainage conditions. Prior to the parametric study, careful model calibration with element tests results and validation against physical modelling tests results were carried out to ensure reliability of the simulations.

2 METHODOLOGY OF NUMERICAL MODELLING

This section summarises the details of the finite element (FE) model to study the uplift behaviour of the suction bucket in sand under a range of drainage conditions using Abaqus (Dassault Systemes, 2020).

2.1 Constitutive model for sand

Apart from the effects of density, confining stress, etc. as captured by the typical critical state-based models, such as the NorSand (Jefferies, 1993), element test results have shown that relative orientation between soil grains and loading direction (referred to as 'fabric anisotropy') also has significant impact on the sand behaviour. Therefore, a critical state based bounding surface plasticity model named SANISAND-F (Petalas et al., 2020) has been employed for modelling the constitutive behaviour of sand. In addtiion to all the functions of the traditional SANISAND model, SANISAND-F is able to macroscopically capture the effects of initial fabric configuration (i.e., sand deposition patterns), and evolution of fabric orientation as a function of loading direction until a critical state is reached.

To achieve this, a dilatancy state parameter, ζ, is introduced in SANISAND-F to adjust the classic state parameter, ψ. This is formulated as:

$$\zeta = \psi - \hat{e}_A\,(e,p)(A-1) \qquad (1)$$

where $\hat{e}_A\,(e,p)$ is a scalar valued function or a positive constant, which controls the magnitude of dilation/contraction for a stress state, and A represents a fabric anisotropy variable (FAV) to account for the influence of fabric $\boldsymbol{F}$ and the direction of plastic strain rate $\boldsymbol{n}'$ during loading, expressed as:

$$A = \boldsymbol{F} : \boldsymbol{n}' \qquad (2)$$

The value of ζ determines whether the soil will exhibit dilative ($\zeta < 0$) or contractive ($\zeta > 0$) behaviour during shearing. By this means, the additional influence of the loading direction and the fabric is captured.

This model has been used previously to investigate the effects of fabric anisotropy on the ultimate capacity of a shallow foundation on dry sand (Chaloulos et al., 2019). However, its performance has not been examined for complex loading scenarios combined with intermediate drainage conditions. This will be described in the following sections.

2.2 Model calibration and validation

In order to validate against the centrifuge modelling tests in da Silva Pereira et al. (2023) in UWA fine silica sand (Table 1), the parameters of the SANISAND-F model were first calibrated against results of drained and undrained triaxial tests on the same sand (Fanni et al., 2022). The tests cover wide range of mean initial confining stresses from 50 to 1000 kPa and relative densities (D_r) from 10% to 80% (Fanni et al., 2022). The calibrated model parameters are summarised in Table 2. Due to space limitation, only one drained and one undrained triaxial tests are selected and plotted on on Figure 1 for comparison.

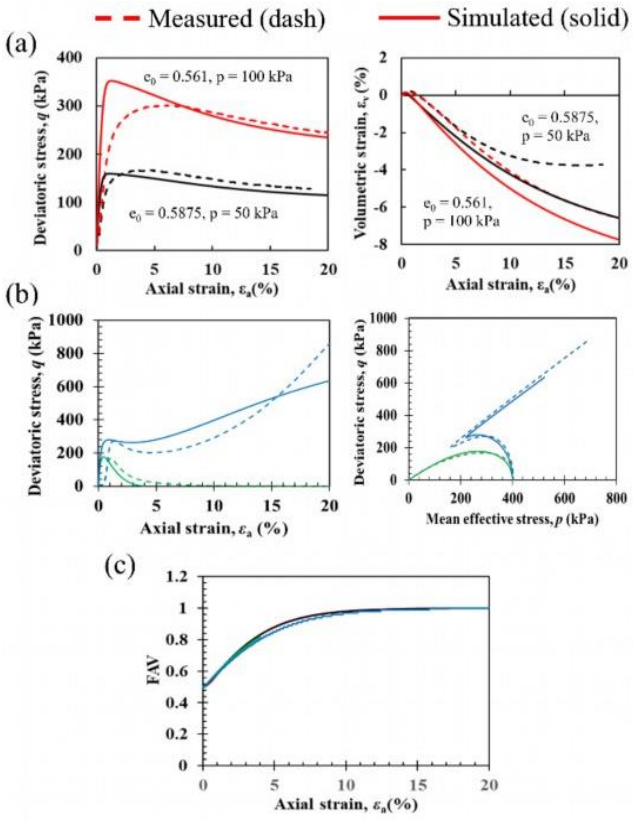

Figure 1. Calibration of SANISAND-F model parameters (a) Drained TXC, (b) Undrained TXC, (c) FAV variation for Drained and Undrained TXC

As shown in Figure 1, good agreement is obtained between the measured and simulated element test responses. At higher strain, FAV value of 1 suggests that critical state has been reached (Figure 1c).

Table 1. Properties of UWA fine silica sand (da Silva Pereira et al., 2023)

Parameters	Value
Specific gravity, G_s	2.67
Median particle size, d_{50}	0.18 mm
Minimum dry density, ρ_{min}	1497 kg/m^3
Maximum dry density, ρ_{max}	1774 kg/m^3
Permeability, k	1×10^{-4} m/s
Critical state friction angle, ϕ_{cs}	31.9º
Coefficient of consolidation, c_v	9×10^{-4} m^2/s for σ'_v ~40 kPa

Table 2. Calibrated parameters of SANISAND-F model for UWA fine silica sand

Parameters	Symbol	Value
Elastic properties	G_0	115
	ν	0.1
Critical state parameters	e_{ref}	0.755
	λ	0.032
	ξ	0.27
	M_c	1.21
	c	0.7
Yield surface size	m	0.01
Plastic modulus controlling parameters	h_1	6.75
	c_h	0.9
	n^b	2.3
Dilation parameters	A_0	0.7
	n^d	2.8
Fabric parameters	e_A	0.06
	F_{in}	0.5
	c_0	10
	h_2	1.1

2.3 Modelling details

Three sets of FE simulations (Table 3) were conducted using an axisymmetric model of a suction bucket-soil system with a bucket having a diameter, *D,* of 8 m, skirt length, *L,* of 4 m and skirt thickness, *t,* of 50 mm, matching the model dimensions used in centrifuge studies by da Silva Pereira et al. (2023). The bucket was 'wished-in-place' in a homogeneous dense fine silica sand, modelled as a rigid body with the reference point at the lid's centre for applying displacement/velocity boundary conditions during pullout.

The soil domain has been discretised with 840 four-noded structured axisymmetric elements. Element type CAX4 is used for Set I analysis and CAX4P for the rest in order to model the effect of excess pore pressures. The elements adjacent to the skirt and below the tip had a size of ~0.01*D* (see Figure 2) to capture the intense interaction between soil and bucket. Interface conditions have been assigned in the model using the "interaction" module in Abaqus based on master and slave surface concept. As the ratio between the average roughness (R_a) of the wall and the median particle size, R_a/d_{50}, is about 0.0028 (da Silva Pereira et al., 2023), the interface friction angle has been selected as 19º (Han et al., 2018).

Table 3. Details of simulations

Set	Details	Purpose
I	Drained analysis (CAX4)	Validation with centrifuge testing
II	Coupled analysis with gap element (CAX4P)	Validation and gain confidence in coupled analysis by comparing with Set I
III	Coupled analysis with gap element (CAX4P)	Parametric study by varying pullout velocity

Based on preliminary studies, both the lateral and bottom boundary has been set at 7.5*D* away from the axis of symmetry and the free surface, respectively (as annotated on Figure 2) to minimize any boundary effects. Radial movements at the side boundary, and both radial and vertical movements at bottom boundary were restricted. Free draining pore pressure boundary condition was adopted at surface for Set II and Set III analyses.

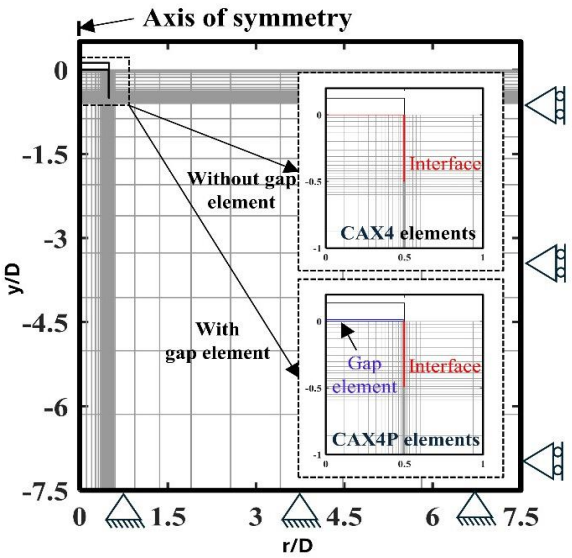

Figure 2. Finite element model prepared in Abaqus

To model generation of the suction pressure and formation of gap during pullout, a thin layer of poroelastic elements, termed 'gap elements', have been introduced between the bucket lid and the top of the soil plug (Figure 2), similar to Achmus and Thieken (2014). The top and bottom of the gap elements are 'tied' to the bucket lid and the top of the soil plug, respectively, i.e., it is not allowed to separate from the

lid or the soil plug. The stiffness of the gap element is kept very low, so that it does not impart any strength on pullout resistance. The permeability of the gap element was set as very high (~10^7 times) than that of the surrounding soil to confirm uniform distribution of excess pore pressure (zero head loss) in the layer during seepage (Maitra et al., 2022). Based on initial sensitivity analyses, it was found that gap elements with a thickness of 0.1 m (~0.012D), a modulus of elasticity of 1 kPa and a Poisson's ratio of 0.01, has minimal influence on the pullout resistance of the bucket. Although not implemented here, adding gap elements below the skirt tip (e.g., Shen et al., 2017) would provide a more realistic model and improve the capture of pullout behavior.

3 VALIDATION OF THE NUMERICAL MODEL

The numerical model was first validated against the centrifuge tests on suction buckets by da Silva Pereira et al. (2023). In tests, after the buckets were installed a vertical pressure of 140 kPa was applied on the bucket prior to being subjected to a parcel of cyclic loads. The bucket was then pulled out at a rate (v) of 0.002 mm/s to ensure a drained condition. Since the peak drained pullout resistance is not affected by the history of the cyclic loading (da Silva Pereira et al., 2023), the cyclic load parcels were not modelled in the analyses.

For Set I, the geostatic pressure is applied first, assuming a coefficient of earth pressure at rest (K_0) of 0.47 (for ϕ_{cs} = 31.9º). It was followed by loading to a vertical pressure of 140 kPa and then full unloading to model what happened in the centrifuge tests. As discussed later, this full cycle of loading changed stress conditions around the bucket and subsequent load-displacement response of the bucket.

In Set II, it was found challenging to apply the vertical load of 140 kPa (as in Set I) due to the gap elements. Therefore, this loading cycle was not modelled and instead, a higher K_0 = 0.6 has been considered for the geostatic conditions. This is supported by the back analysis reported in da Silva Pereira et al. (2023), where they compared their experimental results with the analytical solution by Houlsby and Byrne (2005). Furthermore, examination of the resulting ratio of horizontal to vertical stresses in the vicinity of skirt in Set I suggests the load cycle increased the ratio from the initial value of 0.47 to somewhere between 0.6 and 0.7 locally.

For the final step of both Set I and II analyses, the pullout is modelly by prescribing an upward velocity of v = 0.002 mm/s. The simulated and measured results are shown in Figure 3, with Set I and Set II simulations closely matching the peak pullout resistance from the centrifuge tests. However, a discrepancy in the displacement required to mobilise the peak resistance is observed, likely due to differences in the stress conditions around the bucket before pullout.

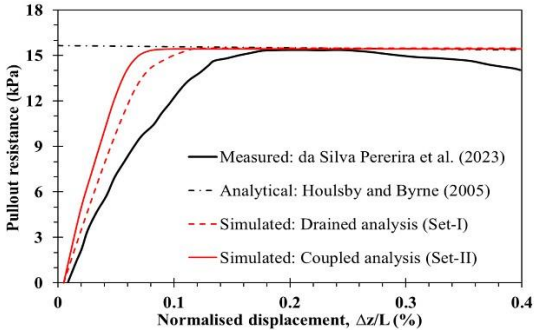

Figure 3. Validation of numerical model

4 PARAMETRIC STUDY ON RESPONSE AT VARIOUS PULLOUT RATES

Following the validations above, a parametric study was performed to quantify the effect of partial drainage on the pullout resistance. The drainage condition is defined using a normalised velocity term of $V = vD/c_v$ (Finnie and Randolph, 1994). For a pullout velocity (v) range of 0.002 mm/s to 20 mm/s, the correponding values of V range from 0.018 to 180. It should be noted that this normalised velocity may not be as suitable for the bucket since the characteristic drainage length depends not only on D, but also L, which is not reflected in the magnitude of V.

4.1 Resistance-displacement response

Variation of the bucket pullout resistance with upward displacement is compared on Figure 4 for different pullout rates. As expected, the pullout resistance increseas with pullout rates. For the slowest rate (V = 0.018), a fully drained response is reached and the pullout resistance is governed by the friction along the inner and outer skirts of the bucket. In comparison, for the highest pullout rate of V = 180, the drainage response is almost undrained, and the resistance is governed by the reverse bearing mechanism mobilised at the base of the soil plug. This is confirmed by the contours of the excess pore pressures near the bucket in Figure 5, and the contours of the mobilised displacements in Figure 6. For the case with the slowest rate, Figure 5a shows that negligible suction was generated below the bucket lid, as the generated negative excess pore pressures have sufficient time to dissipate. Because of this low suction, the soil inside the bucket does not move with the bucket and a gap forms between the bucket lid, which is filled with the

water being sucked in from outside. This behaviour is demonstrated in Figure 7, which shows that the increase in thickness of gap element is almost equal to the normalised displacement of the bucket.

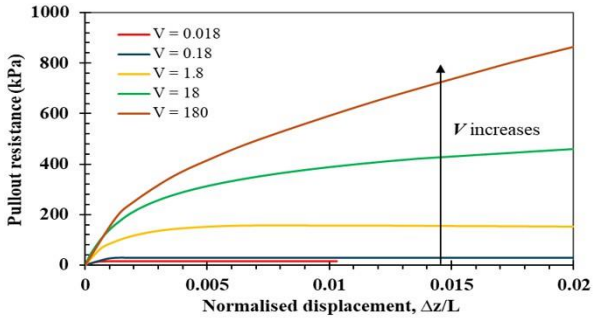

Figure 4. Variation of resistance with pullout rate

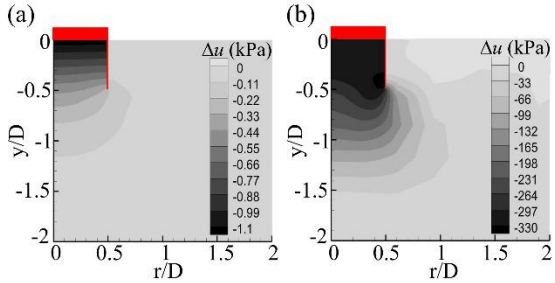

Figure 5. Excess pore pressure (Δu) contours for different pullout rates: (a) V = 0.018 at Δz/L = 0.01; (b) V = 180 at Δz/L = 0.02

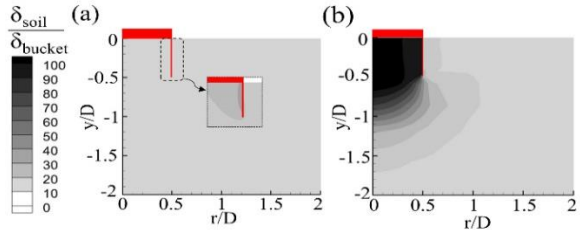

Figure 6. Soil displacement contours for pullout rates: (a) V = 0.018 at Δz/L = 0.01; (b) V = 180 at Δz/L = 0.02

At the highest pullout rate of V = 180, the suction pressure generated within the bucket is very high (Figure 5b). The suction eventually reaches the skirt tip and mobilises the entire soil plug, hence forming a reverse end bearing mechanism (Figure 6b). Similar excess pore pressure contour is also observed in the FE study by Shen et al. (2017). The mechanism is also indicated by the unchanged thickness of the gap element, as shown in Figure 7, suggesting the entire soil plug is being pulled along with the bucket. It is worth noting the pullout resistance is about 2.5 times the suction pressure at $\Delta z/L$ = 0.02, which exceeds the 1.6 to 1.8 ratio observed in the experiments in Houlsby and Bryne (2005), notwithstanding difference in test variables (e.g. L/D, $\Delta z/L$, D_r, k and V). Further work is needed to understand the discrepancy, especially in relation to experimental or field validation data.

For the partially drained condition with intermediate pullout rates, the failure mechanism lies between the two extreme cases mentioned above, as may be expected. Part of the suction pressure is dissipated within the bucket and a partial reverse bearing mechanism governs the pullout resistance.

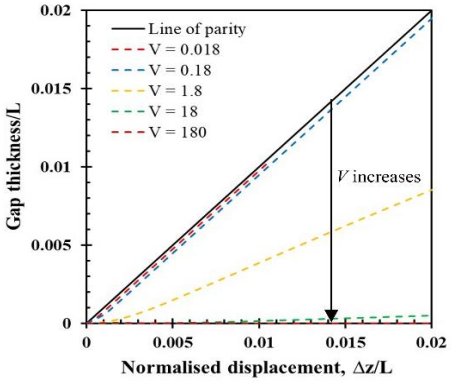

Figure 7. Change in gap thickness with pullout rate

It is important to note that for a particular depth of interest and pullout velocity, the pullout resistance will be limited by the cavitation pressure for that water depth. However, due to software limitations, the effect of cavitation cannot be captured in the present FE model, similar to previous studies (Shen et al., 2017; Achmus and Thieken, 2014).

4.2 Evolution of fabric orientation

Evolution of fabric orientation for a soil element inside and outside the skirt (at mid-height) has been investigated by monitoring the value of FAV when the bucket is being pulled out. The results are shown in Figure 8 for the slowest and fastest pullout rates.

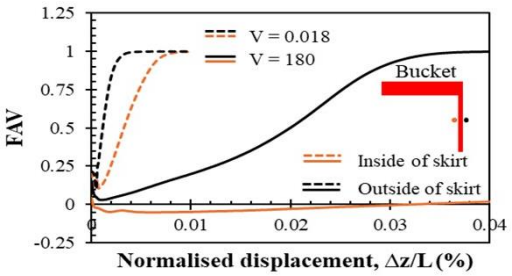

Figure 8. Evolution of FAV parameter with normalised displacement (orange and black lines represent FAV for a soil element inside and outside of the skirt respectively)

For the slowest pullout rate of V = 0.018, the soil adjacent to the skirt is sheared inside and outside the bucket. Because of this, the corresponding value of the FAV changes rapidly and attains its critical value of 1 at small displacements, though requiring somewhat different displacements for the soil element inside and outside the skirt. This may be attributed to the

difference in the soil stiffness and loading directions outside and inside the skirt. For the fastest pullout rate of $V = 180$, the soil plug moves along with the bucket, with little relative movement (or strain) to the skirt. As such, the value of FAV remains almost unchanged for the soil inside the bucket. With increasing $\Delta z/L$, the FAV value for soil element outside the skirt approaches 1.0, albeit at a large normalised displacement as compared to a soil element at the same location for $V = 0.018$.

5 CONCLUSIONS

The pullout behaviour of suction bucket under different drainage conditions has been numerically investigated in this paper. The key observations are:

- The pullout resistance in dense sand increases as pullout rate increases but will be limited by cavitation pressure.
- For drained conditions (corresponding to low *V)*, the uplift resistance is only contributed by the friction along the skirt-soil interface. For undrained conditions (corresponding to high *V)*, reverse end bearing mechanism is mobilised at the base of the soil plug, in addition to the resistance mobilised along the outside of the bucket. Under partially drained conditions (with intermediate *V*), the reverse end bearing mechanism is only partially mobilised. The resistance is a function of the suction generated inside the bucket, which ultimately depends on the dilatancy of the sand and uplift velocity of the bucket against the speed of the water being sucked into the bucket (i.e. dissipation of negative excess pore pressures).
- Additionally, via the value of FAV, evolution of the fabric orientation as the foundation is loaded to failure can be demonstrated to some extent.
- The modelling approach has the potential for predicting the uplift behaviour of the bucket foundation under more complex tensile loading conditions.

AUTHOR CONTRIBUTION STATEMENT

D. Bhakta: Writing- Original draft, Validation, Formal Analysis. **A. Roy**: Writing- Review & Editing, Supervision, Visualization. **S.H. Chow**: Writing- Review & Editing, Supervision, Visualization. **H. Zhou**: Writing- Review and Editing.

ACKNOWLEDGEMENTS

The first author is grateful for financial support (Maitri scholarship) provided by The Centre for Australia-India Relations and Melbourne Research Scholarship.

REFERENCES

Achmus, M. and Thieken, K. (2014). Numerical simulation of the tensile resistance of suction buckets in sand. *J. Ocean and Wind Energy*, 1(4): 231–239.

Ayyılmaz, B., Ülker, M.B.C., Galavi, V. and Barari, A. (2023). Numerical modeling of the effect of loading rate on the tensile load capacity of offshore caisson foundations. *Ocean Eng.*, *284*, 115155.

Chaloulos, Y.K., Papadimitriou, A.G. and Dafalias, Y.F. (2019). Fabric effects on strip footing loading of anisotropic sand. *J. Geotech. Geoenviron. Eng.*, 145(10), 04019068.

da Silva Pereira, F., Bienen, B. and O'Loughlin, C.D. (2023). Mind the gap–an experimental study on the need for grouting suction buckets in sand under vertical cyclic loading. *Géotechnique*, 1–16.

Dassault Systèmes (2020). Abaqus 6.20 analysis user's manual. Dassault Systèmes.

Fanni, R., Reid, D. and Fourie, A. (2022). Effect of principal stress direction on the instability of sand under the constant shear drained stress path. *Géotechnique*, 1–17.

Finnie, I.M.S. and Randolph, M. (1994). Punch-through and liquefaction induced failure of shallow foundations on calcareous sediments. *Proc. of the 7th Int. Conf. on the Behaviour of Offshore Structures* (217–230). Pergamon.

Gütz, P. and Achmus, M. (2021). Suction bucket foundations under cyclic tensile loading–physical and numerical modeling. *Geotechnical Testing J.*, 44(3): 756–781.

Han, F., Ganju, E., Salgado, R. and Prezzi, M. (2018). Effects of interface roughness, particle geometry, and gradation on the sand–steel interface friction angle. *J. Geotech. Geoenviron. Eng.*, *144*(12), 04018096.

Houlsby, G.T. and Byrne, B.W. (2005). Design procedures for installation of suction caissons in sand. *Proc. of the Institution of Civil Engineers-Geotechnical Engineering*, *158*(3), 135-144.

Houlsby, G.T., Kelly, R.B. and Byrne, B.W. (2005). The tensile capacity of suction caissons in sand under rapid loading. *Proc. of the Int. Symp. on Frontiers in Offshore Geomechanics, Perth* (405–410).

Jefferies, M.G. (1993). NorSand: a simple critical state model for sand, *Géotechnique*, 43: 91-103.

Maitra, S., Chatterjee, S., White, D. and Choudhury, D. (2022). Uplift resistance of buried pipelines: The contribution of seepage forces. *Ocean Eng.*, 250, 111037.

Petalas, A.L., Dafalias, Y.F. and Papadimitriou, A.G. (2020). SANISAND-F: Sand constitutive model

with evolving fabric anisotropy. *Int. J. Solids and Structures*, 188: 12–31.

Senders, M. (2008). *Suction Caissons in Sand as Tripod Foundations for Offshore Wind Turbines*. Ph.D thesis, The University of Western Australia, Australia.

Shen, K., Zhang, Y., Klinkvort, R.T., Sturm, H., Jostad, H.P., Sivasithamparam, N. and Guo, Z. (2017). Numerical simulation of suction bucket under vertical tension loading. *Proc. of the 8th Int. Conf. on Offshore Site Investigation and Geotechnics, London, UK*.